Position Control Performance Improvement of DTC-SVM for an Induction Motor: Application to Photovoltaic Panel Position

Fatma Ben Salem[*‡], Nabil Derbel[*]

[*]Control & Energy Management Laboratory (CEMLab) University of Sfax, Sfax Engineering School, BP 1173, 3038 Sfax, Tunisia

(fatma_bs@yahoo.fr, fatma.bensalem@enis.rnu.tn, n.derbel@enis.rnu.tn)

[‡]Corresponding Author: Fatma Ben Salem; e-mail: fatma_bs@yahoo.fr

Received: 29.08.2014 Accepted: 13.10.2014

Abstract- This paper deals with the adaptive sliding mode control DTC-SVM approach dedicated to the position control of photovoltaic panels according to the maximum sunshine position to allow a high efficiency of photovoltaic systems. The paper is devoted to the presentation of a comparison study between three DTC-SVM strategies applied to the position control of an induction motor: (i) a DTC-SVM strategy using PI controllers, (ii) a DTC-SVM strategy using PI controllers with a nonlinear compensator, and (iii) a DTC-SVM strategy using sliding mode controllers. It has been found that a reduction of the flux and the torque ripples, as well as the stator current distortion, have been gained going from the first strategy to the third one. These affirmations are proved by numerical index criteria, such as the torque ripple, the flux ripple and the total harmonic distortion of stator currents. Furthermore, and using an adaptive estimator of motor parameters, the robustness with respect to parameter variations of the induction motor is also tested. These performances are confirmed by simulation works.

Keywords—Induction motor, DTC-SVM, Photovoltaic panel position control, Sliding mode control, Torque ripples, Parameter estimations.

1. Introduction

In the middle of 1980's, *Takahashi and* Depenbrock proposed the Direct Torque Control (DTC) for induction machines [1, 2]. The principle of the DTC is based on the selection of voltage vectors from the difference between the reference and the actual values of the torque and the flux linkages. The torque and the flux errors are compared through hysteresis comparators. Recently, the DTC scheme has presented enormous attention in induction motor drive applications. Of particular interest is the application of the DTC for position control applications [3]. The DTC based position control offers attractive performances, especially the high torque at low speed which is required at standstill. However, the conventional DTC strategy suffers from the demagnetization problem at low speeds, from high torque ripples, and the uncontrolled switching frequency. This is due to hysteresis regulators controlling the electromagnetic torque and the stator flux [4, 5]. This can be overcome by using a proper modulation technique. Space Vector Modulation (SVM) which synthesizes any voltage vector lying inside the sextant gives good performances. The DTC of an induction motor using the space vector pulse width a modulation technique has been described in several studies [6, 7, 8, 9, 10, 11, 12]. Switching instants of different space vectors are determined for each sampling period in order to minimize the torque ripple in SVM technique. Within this approach, the paper proposes a SVM-DTC scheme based on the sliding mode controller technique for the position control of an induction machine dedicated to sun tracker photovoltaic panels. In fact, The maximum sunshine position tracking system is intended to assess as accurately as possible the location of the sun with respect to earth during the day. A proposed tracking system has two freedom degrees in such a way that it allows the displacement of the photovoltaic system within latitudes and meridians: the first degree of freedom is controlled automatically by an induction motor drive under the control of a DTC-SVM

strategy. It allocates the rotation of the photovoltaic panels with an angle variation between −60° and 60°, considering that the 0° angle corresponds to an horizontal position of the photovoltaic panel. The second degree of freedom is achieved according to the period of the year, taking into account of the geographical site in which is located the photovoltaic panel. In what follows, the paper will be focused on the study of the first freedom degree. Within this study, a particular attention is paid to the implementation of a robust DTC-SVM approach in the electric motor drive [13].

Through simulation works, a comparison of performances of a DTC-SVM strategy using PI controllers, and an adaptive sliding mode DTC-SVM strategy dedicated to position control applications is developed. It will be clearly shown that the DTC-SVM based on sliding mode controllers offers best performances. These performances are characterized by a low stator current distortion, the flux and the torque ripples reduction, in transient and steady state response, with the high capability to overcome effects of motor parameters variations.

2. Basic Concept of the DTC-SVM Position Control

Considering a three-phase two-level voltage inverter feeding the induction motor, there are six non-zero voltage vectors and two zero voltage ones which can be applied to the machine terminals. The voltage vectors of the inverter can be expressed as follows:

$$\overline{V}_s = \sqrt{\frac{2}{3}}\left[S_a + S_b e^{j\frac{2\pi}{3}} + S_c e^{j\frac{4\pi}{3}}\right] \quad (1)$$

where S_a, S_b and S_c are the inverter switching functions, which can take logical values 0 or 1.

The stator equation using phase variables can be expressed as:

$$\frac{d}{dt}\overline{\Phi}_s = \overline{V}_s - R_s\overline{I}_s \quad (2)$$

where $\overline{\Phi}_s$, $\overline{V}_s$, $\overline{I}_s$ and R_s are the stator flux, voltage, current and resistance, respectively.

Now, if numerical time varying quantities are considered, and if the voltage drop across the stator resistance is neglected, equation (2) yields:

$$\Delta\overline{\Phi}_s = \overline{\Phi}_s([K+1]T_s) - \overline{\Phi}_s(KT_s) \simeq \overline{V}_s T_s \quad (3)$$

where T_s is the sampling period. This means that the direction of the flux variation is held by the phase voltage.

The stator flux amplitude and the phase are expressed as follows:

$$\begin{cases} \Phi_s &= \sqrt{\phi_{\alpha s}^2 + \phi_{\beta s}^2} \\ \theta_s &= \arctan\left(\dfrac{\phi_{\beta s}}{\phi_{\alpha s}}\right) \end{cases} \quad (4)$$

The electromagnetic torque can be expressed in terms of stator current and flux as:

$$T_{em} = N_p(\phi_{\alpha s} i_{\beta s} - \phi_{\beta s} i_{\alpha s}) \quad (5)$$

where N_p is the pole pair number.

2.1. Position Control Loop Synthesis

For a constant flux $|\Phi_s| = |\Phi_s^*|$, the transmittance binding the torque T_{em} and the speed ω_r is given by [14,15,16]:

$$G(p) = \frac{T_{em}}{\omega_r} = \frac{A}{1+\tau p} \quad (6)$$

where : $\tau = \sigma\frac{L_r}{R_r}$ and $A = N_p\frac{M^2}{R_r L_s^2}|\Phi_s^*|^2$.

Mechanical parts are described by the following equation:

$$J\frac{d\Omega_m}{dt} = T_{em} - T_l \quad (7)$$

where the load torque is expressed by:

$$T_l = K_l \sin\theta \quad (8)$$

State equations of the machine related to the mechanical part become:

$$\begin{cases} \dfrac{d\theta}{dt} &= \Omega_m \\ \dfrac{d\Omega_m}{dt} &= \dfrac{1}{J}T_{em} - \dfrac{K_l}{J}\sin\theta \\ \dfrac{dT_{em}}{dt} &= -\dfrac{1}{\tau}T_{em} + \dfrac{A}{\tau}\omega_r \end{cases} \quad (9)$$

The objective is the design of a suitable controller as described by figure 1.

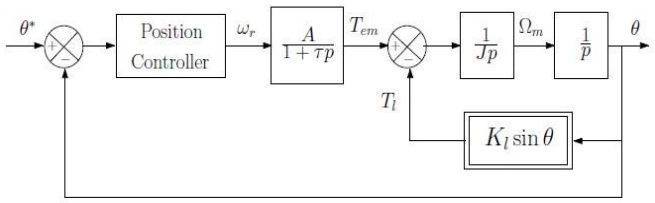

Fig. 1. Position control loop

Fig. 1 shows that the machine part related to the position control contains two cascaded subsystems. The first one translates the electrical part which is represented by the relation between the electromagnetic torque and the rotor pulsation. The second one translates the mechanical part which is represented by the relation between the machine position and the electromagnetic torque.
Then, we have:

$$\begin{cases} \dfrac{d\theta}{dt} &= \Omega_m \\ \dfrac{d^2\theta}{dt^2} &= \dfrac{1}{J}T_{em} - \dfrac{K_l}{J}\sin\ \theta \\ \dfrac{d^3\theta}{dt^3} &= \dfrac{1}{J}\dfrac{dT_{em}}{dt} - \dfrac{K_l}{J}\dfrac{d\theta}{dt}\cos\ \theta \end{cases} \quad (10)$$

This yields:

$$\frac{d^3\theta}{dt^3} = \frac{1}{J}\left(-\frac{1}{\tau}T_{em} + \frac{A}{\tau}\omega_r\right) - \frac{K_l}{J}\frac{d\theta}{dt}\cos\ \theta$$

$$= -\frac{1}{\tau}\left(\frac{d^2\theta}{dt^2} + \frac{K_l}{J}\sin\ \theta\right) + \frac{A}{J\tau}\omega_r - \frac{K_l}{J}\frac{d\theta}{dt}\cos\ \theta \quad (11))$$

Thus, we can write:

$$\frac{d^3\theta}{dt^3} + \frac{1}{\tau}\frac{d^2\theta}{dt^2} + \frac{K_l}{J}\frac{d\theta}{dt} + \frac{K_l}{J\tau}\theta + \varphi\left(\theta, \frac{d\theta}{dt}\right) = \frac{A}{J\tau}\omega_r \quad (12)$$

where:

$$\varphi\left(\theta, \frac{d\theta}{dt}\right) = \frac{K_l}{J}\frac{d\theta}{dt}(\cos\theta - 1) + \frac{K_l}{J\tau}(\sin\theta - \theta) = o\left(\theta, \frac{d\theta}{dt}\right)^3 \quad (13)$$

For small values of θ, $\varphi\left(\theta, \frac{d\theta}{dt}\right)$ can be neglected, and then the mechanical part of the machine can be represented by a third order linear system described by the following transfer function:

$$\frac{\theta}{\omega_r} = \frac{\frac{A}{J\tau}}{\left(p^2 + \frac{K}{J}\right)\left(p + \frac{1}{\tau}\right)} \quad (14)$$

It is to be noted that the application of the following nonlinear feedback represents a nonlinear compensator:

$$\omega_r{}' = \omega_r - \frac{J\tau}{K_l}\,\varphi\left(\theta, \frac{d\theta}{dt}\right) \quad (15)$$

This loop realizes a feedback linearization. The transfer function between θ and $\omega_r{}'$ is expressed as:

$$\frac{\theta}{\omega_r{}'} = \frac{\frac{A}{J\tau}}{\left(p^2 + \frac{K}{J}\right)\left(p + \frac{1}{\tau}\right)} \quad (16)$$

which is an exact transfer function without any approximation.

Observing this transfer function, it is clear that it contains two imaginary poles. This leads to a certain difficulty to control the system with a PID controller $C(p)$:

$$C(p) = K_c\left(1 + \frac{1}{T_i p} + T_d p\right) \quad (17)$$

In fact, the system doesn't present any stability margin. Moreover, to have an adequate dynamical behavior, the derivative time constant T_d should be larger than the integral time constant T_i, which is strongly not recommended.

2.2. Flux Reference Coordinates Computing

The slip angular reference speed ω_r, which is the output of the speed SM controller, will be used to calculate the argument of the stator flux reference. The coordinates of the reference stator flux $\phi^*_{\alpha s}$ and $\phi^*_{\beta s}$ are computed according to the following expressions:

$$\begin{cases} \phi^*_{\alpha s} &= |\Phi^*_s|\cos\theta^*_s \\ \phi^*_{\beta s} &= |\Phi^*_s|\sin\theta^*_s \end{cases} \quad (18)$$

2.3. Voltage Reference Coordinates Computing

The coordinates of the reference voltage vector $V^*_{\alpha s}$ and $V^*_{\beta s}$ in the (α, β) frame is determined by the following equations:

$$\begin{cases} V^*_{\alpha s} &= \dfrac{\phi^*_{\alpha s} - \phi_{\alpha s}}{T_s} + R_s i_{\alpha s} \\ V^*_{\beta s} &= \dfrac{\phi^*_{\beta s} - \phi_{\beta s}}{T_s} + R_s i_{\beta s} \end{cases} \quad (19)$$

These coordinates are introduced into the SVM block, which uses them to control the inverter switches (S_a,S_b,S_c) in each modulation period.

2.4. DTC-SVM Based Position Regulation Scheme

The implementation scheme of a DTC-SVM based position regulation of an induction motor is shown in figure 2. The idea is based on the decoupling between the amplitude and the argument of the stator flux reference vector. The amplitude of this vector will be imposed equal to the nominal value of the stator flux, but the argument will be calculated according to the desired performances. In fact, The error between the reference position θ^* and the measured one θ is applied to the position regulator whose output provides the slip angular reference speed ω_r^*, which will be used to calculate the argument of the stator flux reference. Coordinates of the reference stator flux in the reference frame (α, β) are computed from its polar coordinates according to equations (18). Coordinates of the reference voltage vector $V_{\alpha s}^*$ and $V_{\beta s}^*$ are determined using equations (19). Finally, the SVM block uses these later to generate the convenient stator voltages inverter in each modulation period, ensuring working with a constant commutation frequency.

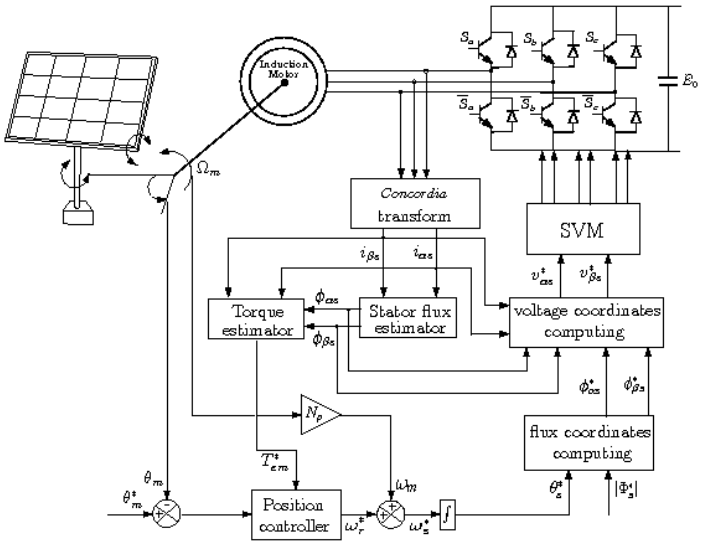

Fig. 2. Induction motor position regulation based on the DTC-SVM strategy.

3. Concept of Sliding Mode Dtc-Svm Based Position Control

Sliding mode (SM) control is well known as variable structure control (VSC) [17,18,19]. Variable structure systems and their associates sliding regimes are characterized by a discontinuous nature of the control action with a desired dynamic of the system which is obtained by an adequate choice of sliding surfaces. Control actions provide the switching between subsystems which give a desired behavior of the closed loop system. For example, consider a nonlinear system described by the following state equation:

$$\dot{X} = f(X) + g(X)U \tag{20}$$

Objectives of the sliding mode control consist of the following steps [17]:

- Design of the switching surface $S(X) \in \mathbb{R}^m$ (m is the dimension of the control U) in order to drive dynamics of the system to evolve on the sliding surface in a reduced time and to remain on this surface. For $S(X) \neq 0$, the following condition: $S(X)^T \dot{S}(X)$ is required to achieve the convergence to the surface $S(X) = 0$. Then, a choice of the sliding surface $S(X)$ can be given by:

$$S(X) = h(X) - h(X^*) \tag{21}$$

with X^* is a reference trajectory.

- Determine a switching control strategy:

$$U = \begin{cases} +U_0 > 0 & \text{if} \quad S(X) < 0 \\ -U_0 < 0 & \text{if} \quad S(X) > 0 \end{cases} \tag{22}$$

- Reduce the chattering phenomenon due to discontinuous nature of the control by using a smooth design function instead of relay control function [19].

In order to decide a system trajectory, the equivalent control U_{eq} represents the required control to reach and to remain on the sliding surface. The corrected term ΔU is required to guarantee the remaining on the surface $S(X) = 0$.

Thus, one can choose for the controller the following expression:

$$U = U_{eq} + \Delta U \tag{23}$$

The equivalent control can be designed as follows: when the system remains on the sliding surface, we have $S(X) = 0$, then $\dot{S}(X) = 0$. Since:

$$\begin{aligned} \dot{S}(X) &= h_1(X)[f(X) + g(X)U] - h_1(X^*)\dot{X}^* \\ &= \mathcal{F}(X, X^*) + \mathcal{G}(X)U \end{aligned} \tag{24}$$

where $h_1(X) = \frac{dh}{dX}$.

This yields the following expression of the equivalent control:

$$\begin{aligned} U_{eq} &= [h_1(X)g(X)]^{-1}\left[h_1(X^*)\dot{X}^* - h_1(X)f(X)\right] \\ &= -[\mathcal{G}(X)]^{-1}\mathcal{F}(X,X^*) \end{aligned} \quad (25)$$

under the regularity of matrix $\mathcal{G}(X) = [h_1(X)g(X)]$.

The term ΔU can be expressed as:

$$\Delta U = -U_0 \ \text{sign}[\mathcal{G}^T(X)S(X)] \quad (26)$$

In fact, if we consider the Lyapunov function $V(X) = S^T S > 0$, its differential with respect to time is expressed as:

$$\dot{V} = S^T\dot{S} = S^T\mathcal{G}(X)\Delta U = -S^T\mathcal{G}(X)\ \text{sign}\left[\mathcal{G}^T(X)S(X)\right] < 0$$

This yields that the closed loop system is stable.

3.1. Position Sliding Mode Controller

The synthesis of the position SM controller, introduced in the position control loop, is designed as follows:

The sliding surface is expressed as:

$$S_\theta = \left(\frac{d}{dt} + \lambda_1\right)^2 \varepsilon_\theta = 0 \quad (27)$$

that is to say:

$$S_\theta = \frac{d^2\varepsilon_\theta}{dt^2} + 2\lambda_1\frac{d\varepsilon_\theta}{dt} + \lambda_1^2\varepsilon_\theta = 0 \quad (28)$$

with: $\varepsilon_\theta = \theta - \theta^*$. This choice takes into account that the error decreases exponentially after reaching the sliding surface. In fact, if $S_\theta = 0$, for $t \geq t_0$, we have: $\varepsilon_\theta(t) = \{\varepsilon_\theta(t_0) + [\dot{\varepsilon}_\theta(t_0) + \lambda_1\varepsilon_\theta(t_0)](t - t_0)\}e^{-\lambda_1(t-t_0)}$

In this case, function $h(X)$ is expressed as:

$$h(X) = \frac{1}{J}T_{em} + 2\lambda_1\Omega_m + \lambda_1^2\theta - \frac{K_l}{J}\sin\theta \quad (29)$$

To remain the state of the system on the sliding surface $S_\theta = 0$, we have: $\dot{S}_\theta = 0$. This leads to:

$$\dot{S}_\theta = \frac{d^3\varepsilon_\theta}{dt^3} + 2\lambda_1\frac{d^2\varepsilon_\theta}{dt^2} + \lambda_1^2\frac{d\varepsilon_\theta}{dt} = 0 \quad (30)$$

That is to say:

$$\begin{aligned} \dot{S}_\theta = \frac{1}{J}\left(-\frac{1}{\tau}T_{em} + \frac{A}{\tau}U\right) + 2\lambda_1\left(\frac{1}{J}T_{em} - \frac{K_l}{J}\sin\theta\right) \\ + \left(\lambda_1^2 - \frac{K_l}{J}\cos\theta\right)\Omega_m - h_1(X^*)\dot{X}^* = 0 \end{aligned} \quad (31)$$

where:

$$h_1(X^*)\dot{X}^* = \left(\ddot{\Omega}_m^* + 2\lambda_1\dot{\Omega}_m^* + \lambda_1^2\dot{\theta}^*\right) \quad (32)$$

Then, it is easy to express the so-called equivalent control which corresponds to the required control remaining the system on the sliding surface:

$$U_{eq,1} = \left[\frac{1}{A}T_{em} - 2\frac{\lambda_1\tau}{A}(T_{em} - K_l\sin\theta) - \frac{J\tau}{A}\lambda_1^2\Omega_m + \frac{\tau K_l}{A}\Omega_m\cos\theta + \frac{J\tau}{A}h_1(X^*)\dot{X}^*\right] \quad (33)$$

Then, the slip angular reference speed ω_r can be expressed by:

$$\omega_r = U_{eq,1} - U_{0,1}\ \text{sign}\ (S_\theta) \quad (34)$$

3.2. Flux Sliding Mode Controller

The synthesis of the sliding mode controller of the stator flux consists in these following stages.

The choice of the sliding surface is given by:

$$S_\phi = (\Phi_s - \Phi_s^*) + \lambda_2\int(\Phi_s - \Phi_s^*)dt \quad (35)$$

where: $\Phi_s^* = |\Phi_s|e^{i\theta_s^*}$ and $|\Phi_s| = \Phi_N = 1Wb$.

Similarly to the last case, and imposing $S_\phi = 0$, the expression of the equivalent control is:

$$U_{eq,2} = R_sI_s + \dot{\Phi}_s^* - \lambda_2(\Phi_s - \Phi_s^*) \quad (36)$$

This leads to the reference stator voltage control:

$$V_s^* = U_{eq,2} - U_{0,2}\ \text{sign}\ (S_\phi) \quad (37)$$

The control loop of the flux is presented in Figure 3.

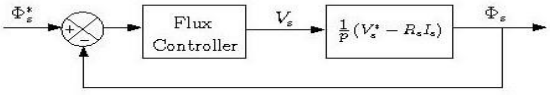

Fig. 3. Flux control loop

The new structure of this control approach is given by the block diagram of figure 4 when we use two sliding mode controllers: one for the position and one for the flux, instead of the PI position controller and the bloc of voltage coordinates computing, used in the basic DTC-SVM strategy based position control of an induction motor.

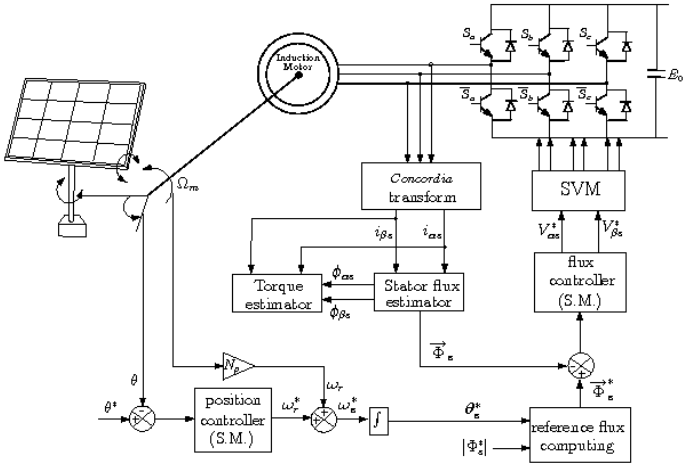

Fig. 4. Induction motor position regulation based on the DTC-SVM with sliding mode controllers

4. Sliding Mode Controllers with Adaptive Parameter Estimation

If system (20) depends on an unknown parameter vector $\gamma = [\gamma_1\ \gamma_2 \dots]^T$, the expression of the control depends on γ, that is to say: $U_{eq} = U_{eq}(\gamma)$ and the applied control law becomes:

$$\overline{U} = \overline{U}_{eq} + \Delta U \tag{38}$$

where $\overline{U}_{eq} = U_{eq}(\overline{\gamma})$. $\overline{\gamma}$ is the estimated vector of γ.

Referring to equation (7), the differential of S is expressed as:

$$\dot{S} = \mathcal{F}(X,X^*) + \mathcal{G}(X)\overline{U} = \mathcal{F}(X,X^*) + \mathcal{G}(X)(\overline{U}_{eq} + \Delta U)$$

$$= \underbrace{\mathcal{F}(X,X^*) + \mathcal{G}(X)U_{eq}}_{=0} + \mathcal{G}(X)\Delta U + \mathcal{G}(X)(\overline{U}_{eq} - U_{eq})$$

$$= \mathcal{G}(X)\Delta U + \mathcal{G}(X)(\overline{U}_{eq} - U_{eq})$$

$$= \mathcal{G}(X)\Delta U + \overline{\mathcal{G}}(X)(\overline{U}_{eq} - U_{eq}) + \underbrace{[\mathcal{G}(X) - \overline{\mathcal{G}}(X)]}_{=o(\Delta\gamma)}\underbrace{(\overline{U}_{eq} - U_{eq})}_{=o(\Delta\gamma)}$$

$$= \mathcal{G}(X)\Delta U + \overline{\mathcal{G}}(X)\left(\sum_i \frac{\partial U_{eq}}{\partial \gamma_i}(\overline{\gamma})\Delta\gamma_i\right) + o(\Delta\gamma)^2$$

$$= \overline{\mathcal{G}}(X)\Delta U + \overline{\mathcal{G}}(X)\left(\sum_i \frac{\partial U_{eq}}{\partial \gamma_i}(\overline{\gamma})\Delta\gamma_i\right) + [\mathcal{G}(X) - \overline{\mathcal{G}}(X)]\Delta U + o(\Delta\gamma)^2$$

$$= \overline{\mathcal{G}}(X)\Delta U + \overline{\mathcal{G}}(X)\left(\sum_i \frac{\partial U_{eq}}{\partial \gamma_i}(\overline{\gamma})\Delta\gamma_i\right) + \left(\sum_i \frac{\partial \mathcal{G}(X)}{\partial \gamma_i}\Delta U\Delta\gamma_i\right) + o(\Delta\gamma)^2$$

$$= \overline{\mathcal{G}}(X)\Delta U + \left(\sum_i \left[\overline{\mathcal{G}}(X)\frac{\partial U_{eq}}{\partial \gamma_i}(\overline{\gamma}) + \frac{\partial \mathcal{G}(X)}{\partial \gamma_i}\Delta U\right]\Delta\gamma_i\right) + o(\Delta\gamma)^2 \tag{39}$$

with $\Delta\gamma = \overline{\gamma} - \gamma$ and $\overline{\mathcal{G}}(X)$ is the expression of $\mathcal{G}(X)$ for $\gamma = \overline{\gamma}$.

- Theorem

Control laws (23), (25) and (26) with the following adaptive laws:

$$\dot{\overline{\gamma}}_i = -\eta_i S^T\left(\overline{\mathcal{G}}(X)\frac{\partial U_{eq}}{\partial \gamma_i}(\overline{\gamma}) + \frac{\partial \mathcal{G}(X)}{\partial \gamma_i}\Delta U\right) \tag{40}$$

stabilise system (20).

- Proof

Let us consider the following Lyapunov function:

$$V = \frac{1}{2}S^T S + \frac{1}{2}\sum_i \frac{1}{\eta_i}\Delta\gamma_i^2 \tag{41}$$

In the following, it assumed that vector γ is constant or it has slow variations with respect to time, in such a way that we can neglect its differential with respect to time: $\dot{\gamma} \simeq 0$. Then, we can write: $\Delta\dot{\gamma} \simeq \dot{\overline{\gamma}}$.

Then, the differential with respect to time of function V is expressed as:

$$\dot{V} = S^T\dot{S} + \sum_i \frac{1}{\eta_i}\Delta\gamma_i\Delta\dot{\gamma}_i$$

$$= S^T\left[\overline{\mathcal{G}}(X)\Delta U + \left(\sum_i \left[\overline{\mathcal{G}}(X)\frac{\partial U_{eq}}{\partial \gamma_i}(\overline{\gamma}) + \frac{\partial \mathcal{G}(X)}{\partial \gamma_i}\Delta U\right]\Delta\gamma_i\right) + o(\Delta\gamma)^2\right] + \sum_i \frac{1}{\eta_i}\Delta\gamma_i\Delta\dot{\gamma}_i + o(\Delta\gamma)^2$$

$$= S^T\overline{\mathcal{G}}(X)\Delta U + \sum_i \underbrace{\left[S^T\left(\overline{\mathcal{G}}(X)\frac{\partial U_{eq}}{\partial \gamma_i}(\overline{\gamma}) + \frac{\partial \mathcal{G}(X)}{\partial \gamma_i}\Delta U\right) + \frac{1}{\eta_i}\Delta\dot{\gamma}_i\right]}_{=0}\Delta\gamma_i + o(\Delta\gamma)^2$$

$$= S^T\overline{\mathcal{G}}(X)\Delta U + o(\Delta\gamma)^2 = -S^T\overline{\mathcal{G}}(X)\text{sign}\left[\overline{\mathcal{G}}^T(X)S(X)\right] + o(\Delta\gamma)^2$$

$$= -||\overline{\mathcal{G}}^T(X)S(X)||_1 + o(\Delta\gamma)^2 < 0 \tag{42}$$

where $||\cdot||_1$ is the norm "1" of a vector which corresponds to the sum of absolute values of its components.

4.1. Position Adaptive Sliding Mode Controller with Variations on The Mutual Inductance and The Rotor Resistance

The sensitivity of the DTC-SVM to (i) variations on the magnetic permeability of the stator and rotor cores, and (ii) variations on the rotor resistance, which can vary with time and operating conditions, can be removed by an online estimation of the mutual inductance and the rotor resistance. The adaptive SM of the speed can be derived based on the mutual inductance and the rotor resistance estimations using the *Lyapunov* theorem.

It is easy to show that:

$$U_1 = \overline{U}_{eq,1} - U_{0,1}\ \text{sign}\ (S_\Omega) \tag{43}$$

where:

$$\overline{U}_{eq,1} = -[\overline{\mathcal{G}}(X)]^{-1}\overline{\mathcal{F}}(X,X^*) \tag{44}$$

Then:

$$\begin{aligned}\dot{S}_\theta &= \mathcal{F}(X,X^*) + \mathcal{G}(X)\overline{U}_1 = \mathcal{F}(X,X^*) + \mathcal{G}(X)(\overline{U}_{eq,1} + \Delta U_1)\\ &= \mathcal{F}(X,X^*) + \mathcal{G}(X)U_{eq,1} + \mathcal{G}(X)\Delta U_1 + \mathcal{G}(X)(\overline{U}_{eq,1} - U_{eq,1})\\ &= \mathcal{G}(X)\Delta U_1 + \mathcal{G}(X)(\overline{U}_{eq,1} - U_{eq,1})\end{aligned} \tag{45}$$

- Corollary

The following slip angular reference speed control law stabilizes the speed loop:

$$\omega_r = \overline{U}_{eq,1} - U_{0,1}\ \text{sign}\ (S_\Omega) \tag{46}$$

where $\overline{U}_{eq1} = U_{eq1}(\overline{M},\overline{R}_r)$, and $\overline{M}$ and $\overline{R}_r$ are estimation values of the mutual inductance and the rotor resistance given by the following updating laws:

$$\dot{\overline{M}} = -\eta_{\theta_1}\overline{\mathcal{G}}S_\theta\left(\frac{\partial U_{eq,1}}{\partial M}\right) \tag{47}$$

$$\dot{\overline{R}}_r = -\eta_{\theta_2}\overline{\mathcal{G}}S_\theta\left(\frac{\partial U_{eq,1}}{\partial R}\right) \tag{48}$$

with : η_{θ_1} and η_{θ_2} positive scalars, $\mathcal{G} = \mathcal{G}(M,R_r)$ and $\overline{\mathcal{G}} = \overline{\mathcal{G}}(\overline{M},\overline{R}_r)$ defined in equation (24).

Proof

Considering the following Lyapunov function:

$$V_\theta = \frac{1}{2}S_\theta^2 + \frac{1}{2\eta_{\theta_1}}\Delta M^2 + \frac{1}{2\eta_{\theta_2}}\Delta R_r^2 \tag{49}$$

with $\Delta M = \overline{M} - M$ and $\Delta R_r = \overline{R}_r - R_r$.

The time derivative of the *Lyapunov* function can be expressed as:

$$\dot{V}_\theta = S_\theta\dot{S}_\theta + \frac{1}{\eta_{\theta_1}}\Delta M\Delta\dot{M} + \frac{1}{\eta_{\theta_2}}\Delta R_r\Delta\dot{R}_r \tag{50}$$

or:

$$\overline{U}_{eq,1} - U_{eq,1} = (\overline{M} - M)\left(\frac{\partial U_{eq,1}}{\partial M}\right) + (\overline{R}_r - R_r)\left(\frac{\partial U_{eq,1}}{\partial R_r}\right) + o(\Delta M,\Delta R_r)^2 \tag{51}$$

Moreover:

$$\mathcal{G}(\overline{U}_{eq,1} - U_{eq,1}) = \overline{\mathcal{G}}(\overline{U}_{eq,1} - U_{eq,1}) + o(\Delta M,\Delta R_r)^2 \tag{52}$$

Thereby, equation (50) gives:

$$\begin{aligned}\dot{V}_\theta &= -U_{0,1}\mathcal{G}(X)|S_\Omega| + \Delta M\left[\overline{\mathcal{G}}\left(\frac{\partial U_{eq,1}}{\partial M}\right) + \frac{1}{\eta_{\theta_1}}\Delta\dot{M}\right]\\ &\quad + \Delta R_r\underbrace{\left[\overline{\mathcal{G}}\left(\frac{\partial U_{eq,1}}{\partial R_r}\right) + \frac{1}{\eta_{\theta_2}}\Delta\dot{R}_r\right]}_{=0} + o(\Delta M,\Delta R_r)^2\\ &= -U_{0,1}\mathcal{G}(X)|S_\Omega| + o(\Delta M,\Delta R_r)^2 \le 0\end{aligned} \tag{53}$$

Since $\mathcal{G}(X) > 0$, $\dot{V}_\theta$ is negative. Then, the system is stable.

4.2. Flux Adaptive Sliding Mode Controller With Variations On Stator Resistance

The stator resistance plays an important role and its value has to be known with good precision in order to obtain an accurate estimation of the stator flux [20,21]. Since the motor heating usually causes a considerable increase in windings resistances, online tuning becomes mandatory. To overcome this problem, an online estimation of the stator resistance is proposed. In fact, the adaptive SM of the stator flux can be derived based on the stator resistance estimation using the *Lyapunov* theorem.

- Theorem

The following stator voltage control laws stabilize the flux loop:

$$\begin{cases} V_{\alpha s} &= V_{\alpha s_{eq}} - k_1\ \text{sign}\,(S_{\phi_\alpha})\\ V_{\beta s} &= V_{\beta s_{eq}} - k_2\ \text{sign}\,(S_{\phi_\beta})\end{cases} \tag{54}$$

where:

$$\begin{cases} V_{\alpha s_{eq}} &= \overline{R}_s I_{\alpha s} - \omega_s^*\phi_{\beta s}^* - \lambda_2 S_{\phi_\alpha}\\ V_{\beta s_{eq}} &= \overline{R}_s I_{\beta s} + \omega_s^*\phi_{\alpha s}^* - \lambda_2 S_{\phi_\beta}\end{cases} \tag{55}$$

and along with $\overline{R}_s$ is the estimation value of the stator resistance, given by the following updating law:

$$\dot{\overline{R}}_s = -\eta_\phi \left(S_{\phi\alpha} I_{\alpha s} + S_{\phi\beta} I_{\beta s} \right) \quad (56)$$

with : η_3 a positive scalar.

- Proof

Considering the following Lyapunov function:

$$V_\phi = \frac{1}{2} S_\phi^T S_\phi + \frac{1}{2\eta_\phi} \Delta R_s^2 \quad (57)$$

with $\Delta R_s = \overline{R}_s - R_s$.

The time derivative of the *Lyapunov* function can be expressed as :

$$\begin{aligned} \dot{V}_\phi &= -\lambda_2 (S_{\phi_\alpha})^2 - \lambda_2 (S_{\beta_\alpha})^2 - k_1 |S_{\phi_\alpha}| - k_2 |S_{\beta_\alpha}| \\ &\quad + \underbrace{\left[(S_{\phi_\alpha} I_{\alpha s} + S_{\phi_\beta} I_{\beta s}) + \frac{1}{\eta_\phi} \Delta \dot{R}_s \right]}_{=0} \\ &= -\lambda_2 (S_{\phi_\alpha})^2 - \lambda_2 (S_{\beta_\alpha})^2 - k_1 |S_{\phi_\alpha}| - k_2 |S_{\beta_\alpha}| \leq 0 \end{aligned} \quad (58)$$

Then the system is stable.

5. Case Study Based On Simulation Results

5.1. Obtained Results

The considered induction motor in the simulation has the parameters given in table 1.

Table 1. Induction machine parameters.

R_s = 0.29Ω	Rr = 0.38Ω	M = 47.3mH
$L_s = L_r$ = 50mH	N_p = 2	J = 0.5Kg m^2

Simulation works have been carried out in order to investigate performances of the position control of the induction motor drive under the above-presented DTC-SVM strategies, using PID, PID with a nonlinear compensator and SM controllers. For the sake of comparison, both strategies have been considered in the same induction motor drive using the same implementation conditions, such that:

- an hysteresis band width of the torque regulator $\varepsilon_\tau = 5N.m$ which represents 10% of the rated electromagnetic torque,
- an hysteresis band width of the flux regulator $\varepsilon_\phi = 0.02Wb$ which represents 2% of the rated stator flux,
- a reference stator flux Φ_s^* equal to $1Wb$,
- The commutation frequency has been kept constant equal to $F_c = 6.25$ kHz in the DTC-SVM strategy.

The desired trajectory is defined by smooth variations of the position θ, the speed Ω_m and the torque T_{em} , leading to:

- variations of θ form $-60°$ (morning panel position) to 30° from 0s to 1s,
- constant value of θ equal to 30° from 1s to 1.5s.
- variations of θ form 30° to 60° (afternoon panel position) from 1.5s to 2.5s,
- constant value of θ equal to 60° from 2.5s to 4s.

The analysis of simulation results leads to the following items:

- Figures 5 and 6 present evolutions of the position θ, the speed Ω_m, the torque T_{em}, the flux $|\phi_s|$ and the current $i_{\alpha s}$, using PID controllers (figures indexed by 1), PID controllers with a nonlinear compensator (figures indexed by 2), and SM controllers (figures indexed by 3). It is well obvious that a good tracking has been realized by these control approaches. It is also obvious, that there is no significant difference between results yielded by PID controllers and PID controllers with a nonlinear compensator. This justifies that the nonlinear term $\varphi\left(\theta, \frac{d\theta}{dt}\right)$ can be neglected. Moreover, ripples of the torque, the flux and stator currents are smallest for results given by SM controllers.
- Figures 7 and 8 present the same variable evolutions for variations of machine parameters as: $+100\%$ variations on the stator resistance R_s, $+100\%$ variations on the rotor resistance R_r and -50% variations on the mutual inductance M. It is clear that results, yielded from PID controllers without and with a nonlinear compensator, present important oscillations. However, SM controllers with parameter's updating give same results as in the case where parameters are known and do not vary.
- Thus, the implementation of the DTC-SVM using sliding mode controllers highlights high dynamical performances obtained with the lowest torque ripple, the lowest flux ripple and the lowest current ripple.

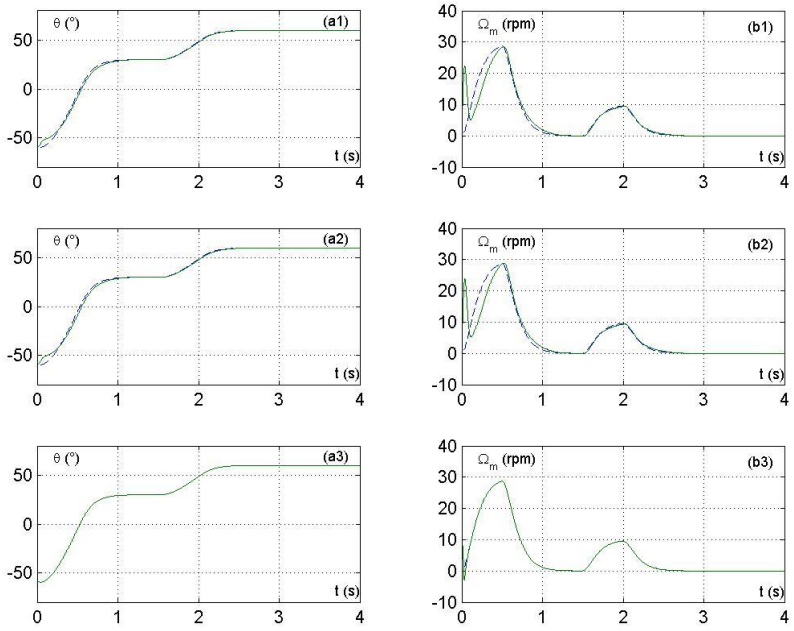

Fig. 5. Induction motor position regulation considering: (subscript "1") DTC-SVM approach using PI controllers, (subscript "2") DTC-SVM approach using PI controllers with a nonlinear compensator, and (subscript "3") DTC-SVM approach using sliding mode controllers. **Legend:** (a) evolution of the actual position and its reference and (b) the speed of the motor and its reference.

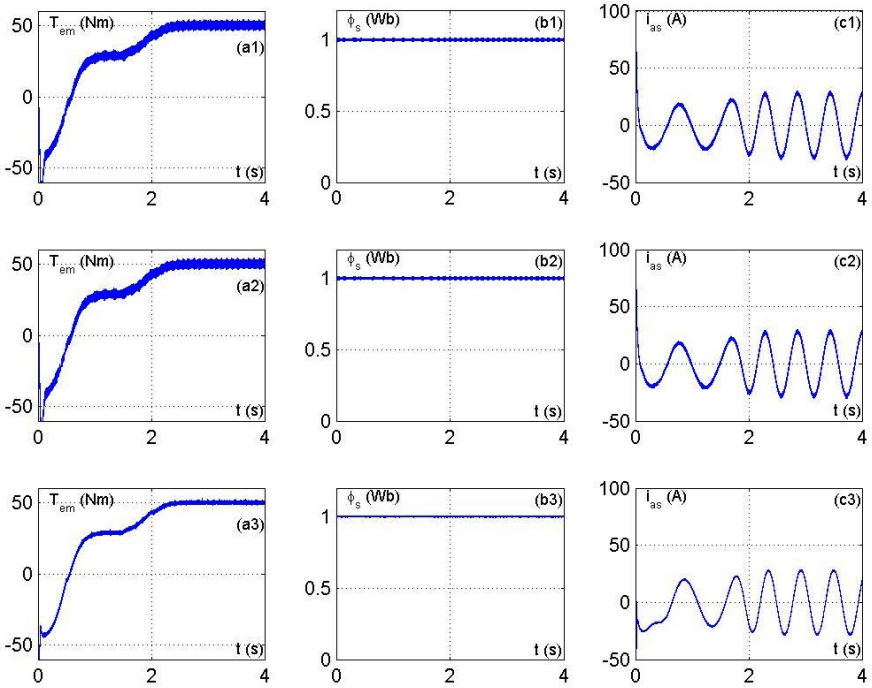

Fig. 6. Induction motor position regulation considering: (subscript "1") DTC-SVM approach using PI controllers, (subscript "2") DTC-SVM approach using PI controllers with a nonlinear compensator, and (subscript "3") DTC-SVM approach using sliding mode controllers. **Legend:** (a) evolution of the electromagnetic torque, (b) the stator flux, and (c) the stator current of phase a**.**

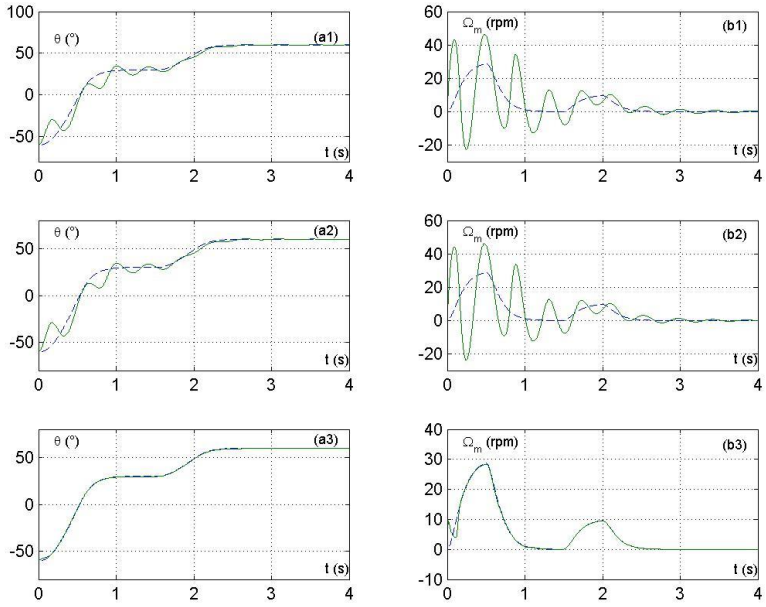

Fig. 7. Induction motor position regulation, with +100% variations on the stator resistance, considering: (subscript "1") DTC-SVM approach using PI controllers, (subscript "2") DTC-SVM approach using PI controllers with a nonlinear compensator, and (subscript "3") DTC-SVM approach using sliding mode controllers. **Legend:** (a) evolution of the actual position and its reference and (b) the speed of the motor and its reference.

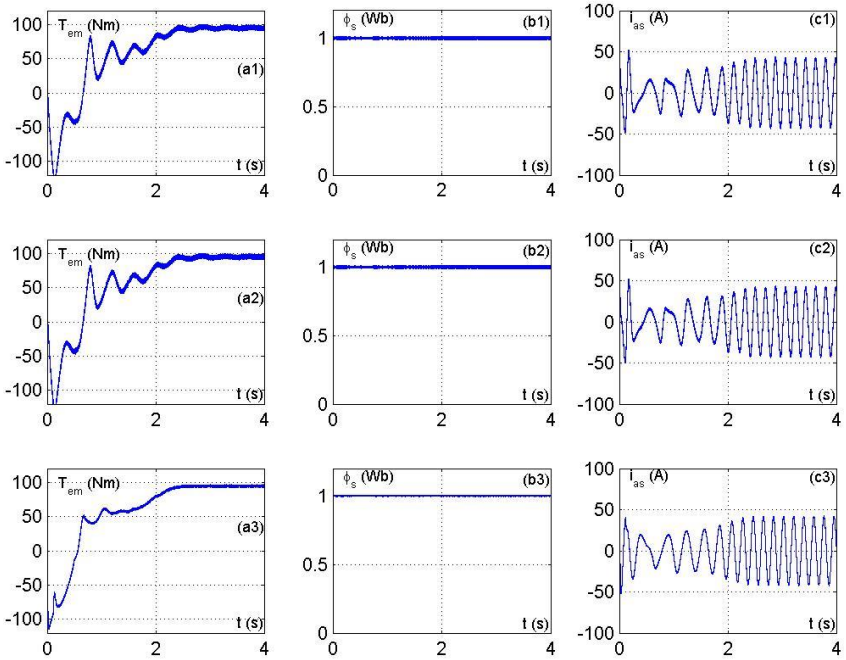

Fig. 8. Induction motor position regulation, with +100% variations on the stator resistance, considering: (subscript "1") DTC-SVM approach using PI controllers, (subscript "2") DTC-SVM approach using PI controllers with a nonlinear compensator, and (subscript "3") DTC-SVM approach using sliding mode controllers. **Legend:** (a) evolution of the electromagnetic torque, (b) the stator flux and (c) the stator current of phase a.

5.2. Performance Criteria

Considering the same simulation, two comparison criteria have been selected to evaluate the effectiveness of the DTC-SVM approaches. First of all, consider the expression of the i_{as} current, around a steady state operating point, as follows:

$$i_{as}(t) = \Re e\left(\sum_{N=1}^{\infty} I_N \exp\left(jN\omega_s t\right)\right) \quad (59)$$

$|I_N|$ is the amplitude of the harmonic N, and $|I_1|$ is the amplitude of the fundamental. In the following, the steady state operating point is defined by a desired position θ equal to 60° for the time larger than 2.5s.

- Total Harmonic Distortion (THD)

The first criterion is the average total harmonic distortion (THD) of the stator current which is defined as follows:

$$\text{THD} = \frac{\sqrt{\sum_{N=2}^{\infty} |I_N|^2}}{|I_1|} \quad (60)$$

In this context, the frequency spectrum of stator current i_{as} has been analyzed. It consists on the observation of amplitudes of all harmonics in terms of harmonic frequencies. The i_{as} frequency spectrum is a representation of current amplitudes I_N as functions of their harmonic ranks N.

Figure 9 shows the evolution of one period of i_{as} between 3s and 4s, its spectrum (only 20 harmonics has been presented). It is obvious that SM controllers give less ripples of the stator current.

The total harmonic distortion criterion of the stator current i_{as} is given by Table 2 which shows that SM controllers give the lowest criterion.

Table 2. Total harmonic distortion of the stator current i_{as}.

	PI without a NL Compensator	PI with a NL Compensator	Sliding Mode Controllers
THD (%)	3.07	3.07	1.23

- Ratio of torque and flux ripples

The second comparison criterion translates the torque and the flux ripples around their steady state values $|\Phi_s| = 1$ and $T_{em,mean} = k_l \sin\frac{\pi}{6}$. They can be expressed as the norm of the ratio of torque or flux ripples by the torque mean or the flux mean, during a certain time period:

$$T_{\text{RIP}} = \left\| \frac{T_{em}(t) - T_{em,mean}}{T_{em,mean}} \right\| = \left\| \frac{T_{em}(t)}{T_{em,mean}} - 1 \right\| \quad (61)$$

$$\Phi_{\text{RIP}} = \left\| \frac{|\Phi_s(t)| - |\Phi_{s,mean}|}{|\Phi_{s,mean}|} \right\| = \left\| \frac{|\Phi_s(t)|}{|\Phi_{s,mean}|} - 1 \right\| \quad (62)$$

Three norms can be considered leading to three criteria describing the torque ripple, based on the three well known norms (the norm 1, the norm 2 and the infinite norm):

$$T_{\text{RIP},1} = \frac{1}{T}\int_{t_0}^{t_0+T} \left| \frac{T_{em}(t) - T_{em,mean}}{T_{em,mean}} \right| dt \quad (63)$$

$$T_{\text{RIP},2} = \sqrt{\frac{1}{T}\int_{t_0}^{t_0+T} \left[\frac{T_{em}(t) - T_{em,mean}}{T_{em,mean}} \right]^2 dt} \quad (64)$$

$$T_{\text{RIP},\infty} = \max_{t_0 \le t < t_0+T} \left| \frac{T_{em}(t) - T_{em,mean}}{T_{em,mean}} \right| \quad (65)$$

and:

$$\Phi_{\text{RIP},1} = \frac{1}{T}\int_{t_0}^{t_0+T} \left| \frac{|\Phi_s(t)| - |\Phi_{s,mean}|}{|\Phi_{s,mean}|} \right| dt \quad (66)$$

$$\Phi_{\text{RIP},2} = \sqrt{\frac{1}{T}\int_{t_0}^{t_0+T} \left[\frac{|\Phi_s(t)| - |\Phi_{s,mean}|}{|\Phi_{s,mean}|} \right]^2 dt} \quad (67)$$

$$\Phi_{\text{RIP},\infty} = \max_{t_0 \le t < t_0+T} \left| \frac{|\Phi_s(t)| - |\Phi_{s,mean}|}{|\Phi_{s,mean}|} \right| \quad (68)$$

T has been chosen equal to the stator period and time t_0 should be chosen in such a way that the system reaches its steady state for t larger than t_0.

Moreover, it is notable that the criterion RIP_2 represents the root-mean-square (RMS) value, and RIP_1 represents the mean absolute (MA) value. However, RIP_∞ represents the maximum ripple (MR) value around the steady state value.

Figure 10 presents the evolution of the torque T_{em} and the flux $|\Phi_s|$ from 3s to 4s. Computations of flux ripple criteria are given by Table 3, and computations of torque ripple criteria are given by Table 4. These tables confirm that the PID controllers without a nonlinear compensator and PID controllers with a nonlinear compensator give same results. However, SM controllers give less ripples of the flux and the torque.

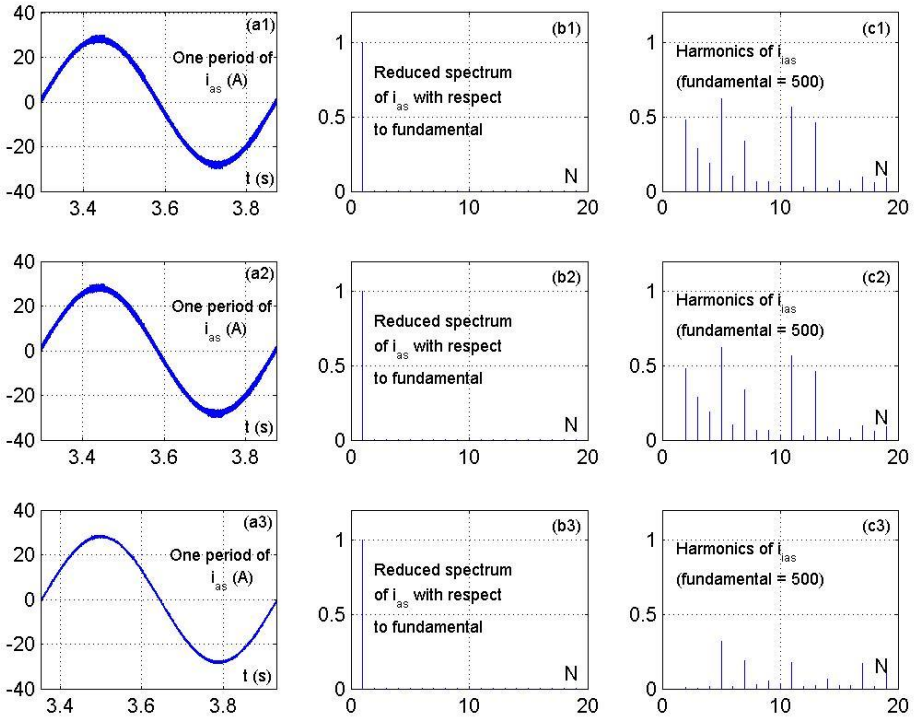

Fig. 9. Spectrum of the current i_{as} : (a) One period of the current i_{as}, (b) Normalized spectrum and (c) Higher harmonics of the spectrum current. (subscript "1") DTC-SVM approach using PI controllers, (subscript "2") DTC-SVM approach using PI controllers with a nonlinear compensator, and (subscript "3") DTC-SVM approach using sliding mode controllers

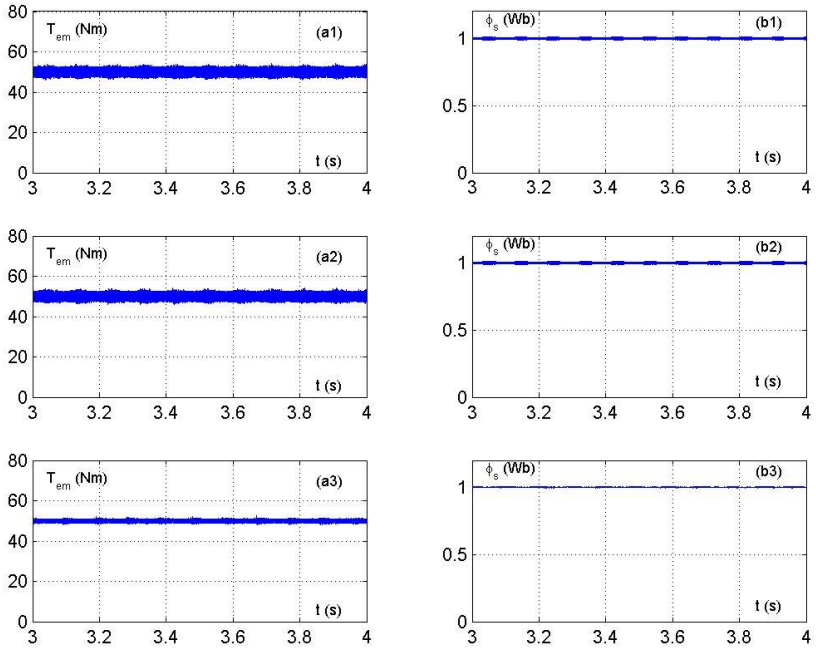

Fig. 10. Zoomed shapes of (a) electromagnetic torque and (b) stator flux. (subscript "1") DTC-SVM approach using PI controllers, (subscript "2") DTC-SVM approach using PI controllers with a nonlinear compensator, and (subscript "3") DTC-SVM approach using sliding mode controllers

Table 3. Flux ripple criteria.

	PI without a NL Compensator	PI with a NL Compensator	SM Controllers
$\Phi_{RIP,1}$ (%)	0.38	0.38	0.12
$\Phi_{RIP,2}$ (%)	0.44	0.44	0.15
$\Phi_{RIP,\infty}$ (%)	1.26	1.33	0.65

Table 4. Torque ripple criteria.

	PI without a NL Compensator	PI with a NL Compensator	SM Controllers
$T_{RIP,1}$ (%)	1.88	1.86	0.92
$T_{RIP,2}$ (%)	2.71	2.66	0.62
$T_{RIP,\infty}$ (%)	8.17	8.34	4.65

6. Conclusion

This paper has been aimed at looking into the presentation and the performance analysis of an adaptive DTC-SVM strategy using sliding mode controllers dedicated to the position control of photovoltaic panels. A comparison study, between the suggested DTC-SVM strategy with PI controllers, with and without a nonlinear compensator, and a DTC-SVM with sliding mode controllers, has been presented. Simulation works have clearly shown that the sliding mode DTC-SVM approach gives best results, lowest ripples on the electromagnetic torque, the stator flux and stator currents. These affirmations have been shown by numerical index criteria, such as the torque ripple, the flux ripple and the total harmonic distortion of stator currents. Moreover, the robustness with respect to parameter variations of the induction motor has been tried on, using updated online estimations of machine parameters.

Acknowledgements

The authors gratefully acknowledge the University of Sfax, Tunisia and the Technology University of Chemnitz for their supports to the success of the present work.

References

[1] I. Takahashi and T. Noguchi, "A New Quick-Response and High-Efficiency Control Strategy of an Induction Motor," IEEE Trans. on Industry Applications, vol. IA-16, no. 4, pp. 820–827, 1986.

[2] M. Depenbrock, U. Baader, G. Gierse, "Direct Self-Control (DSC) of Inverter-Fed Induction Machine: a Basis for Speed Control without Speed measurement", IEEE Trans. on Power Electronics, vol. 3, no.4, pp. 420–429, 1988.

[3] O. Barambones, P. Alkorta and J. M. G. De Durana, "Sliding mode position control for real-time control of induction motors", International Journal of Innovation Computing, Information and Control, vol. 9, no. 7, pp. 2741–2754, 2013.

[4] F. Ben Salem, A. Yangui and A. Masmoudi, "On the reduction of the commutation frequency in dtc : a comparative study", European Trans. on Electrical Power Engineering (ETEP). vol. 15, no. 6, pp. 571–584, 2005.

[5] H. I. Okumus and M. Aktas, "Adaptive Hysteresis Band Control for Constant Switching Frequency in Direct Torque Control of Induction Machine Drives", Elec. Eng. & Comp. Sci. , vol 18, no. 1, pp.59-69, 2010.

[6] T. G. Habetler, F. Profumo, M. Pastorelli and L. M. Tolbert. "Direct torque control of induction machines using space vector modulation", IEEE Trans. On Industry Applications, vol. 28, no. 5, pp. 1045–1053, 1996.

[7] C. Y. Chen,. Sliding Mode Controller deseign of Induction Motor Based on Space-Vector Pulsewidth Modulation Method. International Journal of Innovative Computing, Information and Control, vol.5, no.10, pp. 3603-3614, 2009.

[8] S. Belkacem, F. Naceri and R Abdessemed, "A Novel Robust Adaptive Control Algorithm and Application to DTC-SVM of AC Drives", Serbian Journal Of Electrical Engineering, vol. 7, no.1, pp. 21-40, 2010.

[9] S. A. Davari, E. Hasankhan, D.A. Khaburi, "A comparative study of DTC-SVM with three-level inverter and an improved predictive torque control using two-level inverter", 2nd Power Electronics, Drive Systems and Technologies Conference, pp. 379 - 384, 16-17 February, 2011.

[10] A. Joseline Metilda, R. Arunadevi, N. Ramesh and C. Sharmeela, "Analysis of direct torque control using space vector modulation for three phase induction motor", Recent Research in Science and Technology, vol. 3, no7, pp. 37–40, 2011.

[11] H. F. Rashag, S.P. Koh, K.H. Chong, S.K. Tiong, N. M.L. Tan and A. N. Abdalla, "High performance of space vector modulation direct torque control SVM-DTC based on amplitude voltage and stator flux angle", Research Journal of Applied Sciences, Engineering and Technology, vol. 5, no. 15, pp. 3934–3940, 2013.

[12] N. Ahammad, S. A. Khan and R. K. Reddy, "Novel DTC-SVM for an Adjustable Speed Sensorless Induction Motor Drive", International Journal of Science Engineering and Advance Technology (IJSEAT), vol. 2, no.1, pp. 31–36, 2014.

[13] B. Bouzidi, F. Ben Salem, A. Yangui and A. Masmoudi, "Direct Torque Control strategy Based Maximum Sunshine Position Tracking", in CD-ROM Second International Conference and Exhibition on Ecological Vehicles and Renewable Energies, Monte Carlo, Monaco, 4-7 february, 2007.

[14] W. Srirattanawichaikul, Y. Kumsuwan and S. Premrudeepreechacharn, "Reduction of torque ripple in direct torque control for induction motor drives using decoupled amplitude and angle of stator flux control", ECTI Trans. On Electrical Engineering, Electronics, and Communications, vol. 8, no. 2, pp. 187–196, 2010.

[15] A. Ouarda and F. Ben Salem, "Induction Machine DTC-SVM: A Comparison Between Two Approaches" IEEE 10th Int. Conf. on Systems, Signals and Devices (SSD'13), Hammamet, Tunisia, 18-21March, 2013.

[16] F. Ben Salem and N. Derbel, "Direct torque control of induction motors based on discrete space vector modulation using adaptive sliding mode control" accepted for publication in the international journal of Electric Power Components and Systems, Mai 2014.

[17] K. D. Young, V. I. Utkin, U. Ozguner, "A control engineer's guide to sliding mode control", IEEE Trans. Control Syst. Technol. Vol.7, no.3, pp. 328-342, 1999.

[18] M. S. Carmelia, M. Maurib, "Direct torque control as variable structure control: Existence conditions verification and analysis", Electric Power Systems Research. Vol.81, pp. 1188–1196, 2011.

[19] F. Ben Salem and N. Derbe, "A Sliding Mode field Oriented Control of an Induction Machine Operating with Variable Parameters", Journal of Power and Energy Systems, vol. 27, no.1, pp. 205-212, 2007.

[20] F. Zidani and D. Diallo, "Direct Torque Control of Induction Motor With Fuzzy Stator Resistance Adaptation", IEEE Trans. on energy converion, vol. 21, no. 2, pp. 619–621, 2006.

[21] B. Mouli Chandra and Dr S. Tara Kalyani, "FPGA Controlled Stator Resistance Estimation In IVC of IM using FLC", Global Journal of Researches in Engineering Electrical and Electronics Engineering, vol. 13, no. 13, Online ISSN:2249-4596& Print ISSN:0975-5861, 2013.